Supplemental figure legends

Fig. S1 Test antibodies for FACS-based screens, related to Figure 1A.

(A) Plots of single cells based on FITC intensity and PI intensity. Red and blue dots respectively indicate mock and CPT treated samples prepared using HEK293A cells.

(B) Normalized histograms of FITC intensity. Red and blue peaks respectively indicate mock and CPT treated samples prepared using HEK293A cells.

Fig. S2 DrugZ analysis results of 30 screens, related to Figure 1A.

DrugZ analysis of sgRNA abundance between Top and Bottom groups in 30 screens. See also Table S1 and S2.

Fig. S3 Comparison of screen data conducted with pKAP1 and pChk2 antibodies, related to Figure 1B.

(A) DrugZ analysis of sgRNA abundance between Top and Bottom groups in screens obtained with an antibody recognizing endogenous pChk2 in IR- or HU-treated samples.

(B) Venn diagram shows the overlaps of positive regulators in screens obtained with antibodies recognizing endogenous pKAP1 or pChk2 in IR-treated samples.

(C) Immunoblots of indicated proteins using samples prepared from IR-treated HEK293A cells.

Fig. S4 The regulatory network of DNA damage-induced signaling revealed by treatment-based analysis, related to Figures 1C.

(A) The criteria for analyzing positive and negative regulators of DDR signaling based on treatment.

(B) Heatmap plots show the normZ values of hub candidates. Red and blue colors represent positive and negative regulators, respectively. NormZ values were grouped by their absolute values (1 to 2, 2 to 4, and over 4), labelled by different colors.

(C) Representation of the Reactome pathway network for the proteins in A. The network was generated using the Cytoscape plug-in ClueGO. The pathways highlighted in color were significantly enriched. The GO term list is provided in Table S4.

Fig. S5 Distinct positive and negative regulators specifically participate in cellular responses to CPT and ETO treatment, related to Figure 1C.

(A) DrugZ analysis of sgRNA abundance between Top and Bottom groups in screens obtained with an antibody recognizing endogenous γH2AX in CPT- and ETO-treated samples.

(B) Venn diagram shows the overlaps of positive regulators in the indicated screens.

(C) Venn diagram shows the overlaps of negative regulators in the indicated screens.

(D) NormZ scores of hub regulators across the 30 screens, which highlight the specific involvement of unique sets of genes involved in CPT or ETO-induced DDR signaling.

Fig. S6 Identification of common positive regulators involved in DDR signaling, related to Figure 1C.

(A) Venn diagram shows the overlaps of common positive regulators in 24 screens.

(B) DrugZ analysis of screens obtained with an antibody recognizing endogenous pRPA2-S4/S8.

(C) Immunoblots of DDR signaling proteins were conducted with lysis prepared from ALDOA knockdown HEK293A cells or control cells. HEK293A cells were infected with vector or ALDOA-shRNA1/2 virus, followed by treatment with CPT, ETO and HU, and lysed directly with SDS loading buffer for Western blotting analysis using indicated antibodies.

(D) Immunoblots of DDR signaling proteins were conducted with lysis prepared from U2OS cells with or without ALDOA knockdown in the presence or absence of DNA damaging agents.

Fig. S7 Two previously unknown proteins C21orf59 and C11orf57 were identified as key regulators of DDR signaling, related to Figures 1A and 2B.

(A) DrugZ analysis of sgRNA abundance in the screen obtained with antibody recognizing CPT-induced pKAP1 sample.

(B) HEK293A cells were co-transfected with constructs encoding C11orf57 and vector or LentiV2-C11orf57-sgRNAs (1-8). 40 hours later, cells were lysed directly for Western blotting. C11orf57 antibody was obtained from Proteintech.

(C) HEK293A cells infected with indicated sgRNAs of C11orf57 and selected by puromycin. Cells were then exposed to 1 μM CPT for 1 h and fixation, followed by staining and flow cytometry analysis.

(D) DrugZ analysis of sgRNA abundance in the screen obtained with antibody recognizing CPT-induced RPA2S33 sample.

(E) Immunoblots of C21orf59 prepared from control and C21orf59 knockdown HEK293A cells were performed with two different commercial antibodies purchased from Proteintech and GeneTex respectively.

(F) HEK293A cells were infected with vector or pGIPZ-C21orf59-shRNA2/4/6. After puromycin selection, cells were exposed to 1 μM CPT for 1 h and fixed, followed by staining and flow cytometry analysis.

Fig. S8 C21orf59 may regulate pRPA2S33 via its effect on DNA replication, related to Figure 2B.

(A, B) Immunoblots of DDR signaling proteins were conducted with lysates prepared from control and C21orf59 knockdown HEK293A cells. HEK293A cells were infected with empty virus (vector) or virus expressing C21orf59-shRNA2/6, followed by treatment with CPT (1 μM) or DMSO (i.e. no treatment; NT), and (A) lysed directly with SDS loading buffer for Western blotting analysis using indicated antibodies; (B) NETN buffer extraction to isolate soluble fraction (SF) and the remaining pellet was further treated with TurboNuclease to isolate chromatin fraction (CF). The whole cell lysates (WCLs) were prepared separately using the same samples. Immunoblots of the indicated proteins were conducted. Anti-Vinculin and anti-H3 were respectively included as the loading control for soluble and chromatin fractions.

(C) Cells were infected with indicated viral particles and pulse labelled with 10 μM EdU for 30 min. Representative images of EdU immunostaining in control and C21orf59 knockdown cells were shown (left panel; scale bar 100 px). More than 100 cells were counted for the analysis (right panel). Data are represented as mean ± SEM. n= 3 biological independent replicates. Two-tailed unpaired t test with Welch's correction was used for statistical analysis.

(D) HEK293A cells were treated with CPT (1 μM or 5 μM) or DMSO, followed by NETN buffer extraction to isolate soluble fraction (SF) and the remaining pellet was further treated with TurboNuclease to isolate chromatin fraction (CF). The whole cell lysates (WCLs) were prepared separately using the same samples. Immunoblots of the indicated proteins were conducted. Anti-Vinculin and anti-H3 were respectively included as the loading control for soluble and chromatin fractions.

(E) C21orf59 knockdown cells showed modest sensitivity to HU treatment. HEK293A cells were infected with empty virus or virus encoding C21orf59-shRNA2/6. After puromycin selection, the infected cells were seeded in 96 well-plates overnight and then treated with IR, CPT, ETO, or HU. Cell survival was then determined with the use of CellTiter-Glo luminescence assays. Data are represented as mean ± SEM. n= 6 biological independent replicates.

Fig. S9 The suppressive effect on CPT- and ETO-induced DDR signaling by proteasome inhibition, related to Figures 1D and 3A.

(A) Immunoblots of DDR signaling proteins were conducted with lysates prepared from HeLa and U2OS cells. Cells were pretreated with 10 μM MG132 or DMSO for 1 h and then treated with CPT or ETO.

(B) Proteasome inhibition leads to increased chromatin-bound topoisomerases. HEK293A cells were pretreated with 10 μM MG132 for 1 h and then treated with 1 μM CPT or 10 μM ETO for 2 hours before cells were collected for RADAR assay. Anti-DNA blot was included as the loading control. The quantification was performed with Image J.

(C) Immunofluorescent staining of γH2AX and EdU in HEK293A cells. Cells were pulse labeled with 10 μM EdU for 30 min and washed twice, followed by pre-treatment with 10 μM BTZ for 1 h and treatment with 5 μM or 10 μM CPT for 1 h. Representative images of γH2AX and EdU were shown (scale bar 20 μm).

Fig. S10 The effect of PRMT1 and PRMT5 inhibitors on cell proliferation and HU-induced DDR signaling, related to Figures 2A, 2B and 4A-4D.

(A) PRMT1 inhibitor- or PRMT5 inhibitor-treated cells exhibit defects in cell proliferation. CellTiter-Glo luminescence assay as well as clonogenic assay were used to check cell proliferation when HEK293A cells were treated with PRMT1 inhibitor or PRMT5 inhibitor (1 μM or 10 μM) for the indicated days. Data are represented as mean ± SEM. n= 6 biological independent replicates.

(B) Immunoblots of DDR signaling proteins in lysates prepared from HEK293A cells. Cells were pre-treated with 1 μM or 10 μM PRMT1 inhibitor (EPZ019997) for 3 days followed by HU treatment.

(C) Immunoblots of DDR signaling proteins in lysates prepared from HEK293A cells. Cells were pre-treated with 1 μM or 10 μM PRMT5 inhibitor (EPZ015666) for 3 days followed by HU treatment.

(D) Detecting *ATM* mRNA level in PRMT1 inhibitor- and PRMT5 inhibitor-treated cells by RT-qPCR. HEK293A cells were treated with the indicated concentrations of PRMT1 or PRMT5 inhibitors for 3 days, followed by RT-qPCR with different primers targeting *ATM*. *Actin* was used as the control for the normalization. Data are represented as mean ± SEM. n= 3 biological independent replicates.

Fig. S11 PRMT1 and PRMT5 regulate ATM protein level, related to Figures 4E-4H.

(A) Immunoblots of indicated proteins prepared from PRMT1 or PRMT5 knockdown HEK293A cells.

(B) Immunoblots of indicated proteins prepared from PRMT1 or PRMT5 knockdown U2OS cells.

(C) Treatment of PRMT1 or PRMT5 inhibitor sensitizes cells to DNA damaging agents. HEK293T and U2OS cells were seeded in 96 well-plates with DMSO, PRMT1 inhibitor (1 μM or 10 μM) or PRMT5 inhibitor (1 μM or 10 μM) overnight and then treated with IR, CPT, ETO, or HU. Cell survival was then examined using CellTiter-Glo luminescence assays. Data are represented as mean ± SEM. n= 6 biological independent replicates.

Fig. S12 Identification of GNB1L as the critical regulator of DDR signaling, related to Figure 5A.

(A) DrugZ analysis of sgRNA abundance in screens obtained with antibodies recognizing γH2AX and pKAP1 in CPT- and ETO-treated samples.

(B) Immunofluorescence staining of Flag-tagged GNB1L in HEK293T cells that stably express SFB-GNB1L. Representative images of Flag (SFB-GNB1L) were shown (scale bar 20 μm).

(C) GNB1L-depleted cells exhibit defective cell proliferation. CellTiter-Glo luminescence assay as well as clonogenic assay were used to check cell proliferation when GNB1L-dTAG cells were treated with NEG or dTAG^{V}-1 for the indicated days. Data are represented as mean ± SEM. n= 6 biological independent replicates.

(D) Immunoblots of GNB1L-HA proteins prepared from GNB1L-dTAG cells. GNB1L-dTAG cells were treated with dTAG^{V}-1-NEG or dTAG^{V}-1 for indicated hours. Vinculin was included as the loading control.

(E) Immunoblots of the indicated proteins prepared from GNB1L-dTAG cells treated with dTAG^{V}-1 or dTAG^{V}-1-NEG with time course.

(F) Clonogenic survival of GNB1L-dTAG cells as well as reconstituted GNB1L cells in the presence of dTAG^{V}-1 (1 μM) or dTAG^{V}-1-NEG (1 μM).

Fig. S13 GNB1L specifically regulates PIKK protein levels, but not their mRNA levels, related to Figure 6C.

(A and B) HEK293A-GNB1L-dTAG cells were treated with 1 μM NEG or dTAG^{V}-1 for 3 days followed by the label-free quantitative proteomics analysis (see also Table S5) and RNA-seq (see also Table S6). Volcano plots are presented showing the differentially expressed proteins (A) and genes (B) in dTAG^{V}-1-treated cells comparing to those in NEG-treated cells.

(C) Representative GO terms enriched by differentially expressed genes identified from RNA-seq analysis. The GO term list is provided in Table S6.

Fig. S14 TELO2 depletion recapitulates the effect of depleting GNB1L on PIKK proteins but does not enhance its effect, related to Figure 6F.

(A and B) Validation of two different HEK293A-TELO2-dTAG clones by Western blot (A) and clonogenic survival (B) assays.

(C) TELO2-dTAG cells were treated with 1 μM NEG or dTAG^{V}-1 for indicated days, followed by immunoblots of the indicated proteins.

(D) HEK293A-GNB1L-dTAG cells were treated with 1 μM NEG or dTAG^{V}-1, further infected with LentiV2-sgRNA virus targeting TTI1 or TELO2. The cells were lysed directly after 3 days and immunoblotted for the indicated proteins.

(E) HEK293T cells stably expressing SFB-GNB1L were treated with 10 μM HSP70 inhibitor (VER155008) or HSP90 inhibitor (17-AAG) for 2 h, followed by co-immunoprecipitation assay to identify the interaction between GNB1L and the indicated proteins.

(F) The HEK293A-GNB1L-dTAG cells were reconstituted with GNB1L truncation mutants SFB-GNB1L-ΔWD (1-7) (depleting WD1, residues 16-54; depleting WD2, residues 58-97; depleting WD3, residues 103-145; depleting WD4, residues 153-195; depleting WD5, residues 200-237; depleting WD6, residues 242-282; depleting WD7, residues 286-323) or full-length (FL) GNB1L, followed by treatment with 1 μM NEG or dTAG^{V}-1 for 3 days. Immunoblots of the indicated proteins were presented.

(G) Clonogenic survival of HEK293A-GNB1L-dTAG cells as well as GNB1L reconstituted cells in the presence of 1 μM dTAG^{V}-1-NEG or dTAG^{V}-1.

(H) Co-immunoprecipitation assays were performed with HEK293A-GNB1L-dTAG cells as well as GNB1L reconstituted cells to identify the interaction of GNB1L truncation mutants with the indicated endogenous proteins.

Fig. S15 GNB1L maintains genomic stability, related to Figures 5F and 6B.

(A and B) GNB1L-dTAG cells were treated with 1 μM dTAG^{V}-1-NEG or dTAG^{V}-1 for 3 days. Representative examples of neutral comet assay conducted with NEG- or dTAG^{V}-1-treated GNB1L cells in the absence or presence of ETO treatment (10 μM for 1 h). More than 100 cells of each group were counted for analysis. Two-tailed unpaired t test with Welch's correction was used for statistical analysis. Representative images were shown (scale bar 20 μm).

(C and D) GNB1L-dTAG cells were treated with 1 μM dTAG^{V}-1-NEG or dTAG^{V}-1 for 3 days. Representative examples of mitotic spreads from NEG- or dTAG^{V}-1-treated GNB1L cells (scale bar 20 μm). The red arrows indicate chromosomal fragments. 50 metaphases were counted for analysis and cells with 2 or more chromosomal fragments were counted as aberrations.

Fig. S16 The correlation of GNB1L expression in cancers, related to Figures 5F and 6B.
(A) Boxplots show the expression distribution (log2(tpm+0.001)) of GNB1L gene in tumor tissues and normal tissues. The abscissa represents different tumor tissues, and the ordinate represents the expression distribution of GNB1L, different colors represent different groups. RNA-sequencing expression (level 3) profiles for GNB1L were downloaded from the TCGA dataset (https://portal.gdc.com).
(B) Kaplan-Meier survival analysis of the GNB1L from TCGA dataset. For each tumor type, patients were divided into a low group (lower expressed GNB1L) and a high group (higher expressed GNB1L) by the median expression of GNB1L. The high and low groups were stratified and visualized using Kaplan-Meier survival curves and analyzed for statistical significance using the log-rank test and univariate cox regression analysis. RNA-sequencing expression (level 3) profiles and corresponding clinical information for GNB1L were downloaded from the TCGA dataset (https://portal.gdc.com).

Fig. S1

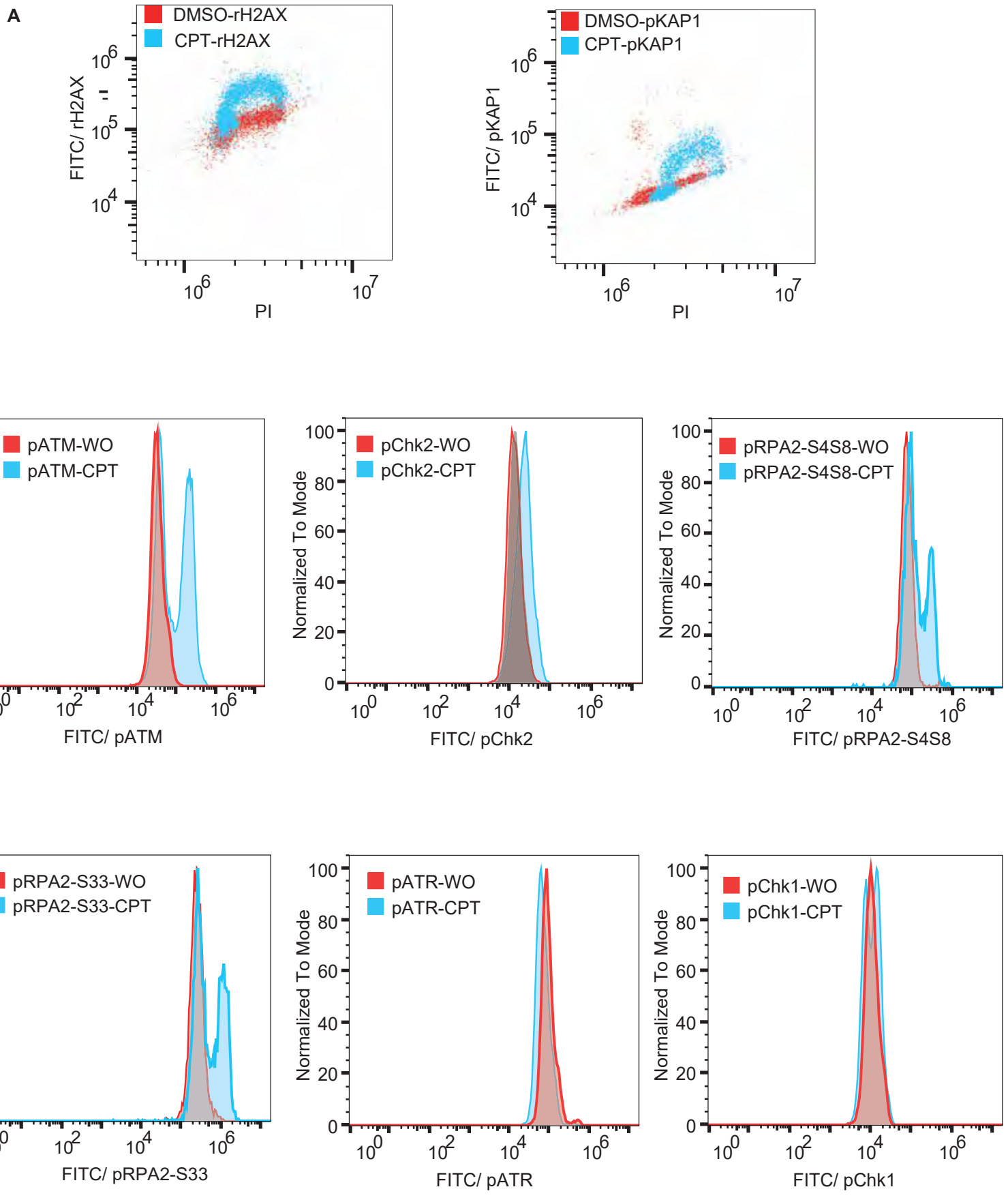
A
DMSO-rH2AX
CPT-rH2AX
FITC/ rH2AX
PI
DMSO-pKAP1
CPT-pKAP1
FITC/ pKAP1
PI
B
pATM-WO
pATM-CPT
Normalized To Mode
FITC/ pATM
pChk2-WO
pChk2-CPT
FITC/ pChk2
pRPA2-S4S8-WO
pRPA2-S4S8-CPT
FITC/ pRPA2-S4S8
pRPA2-S33-WO
pRPA2-S33-CPT
FITC/ pRPA2-S33
pATR-WO
pATR-CPT
FITC/ pATR
pChk1-WO
pChk1-CPT
FITC/ pChk1

Fig. S2

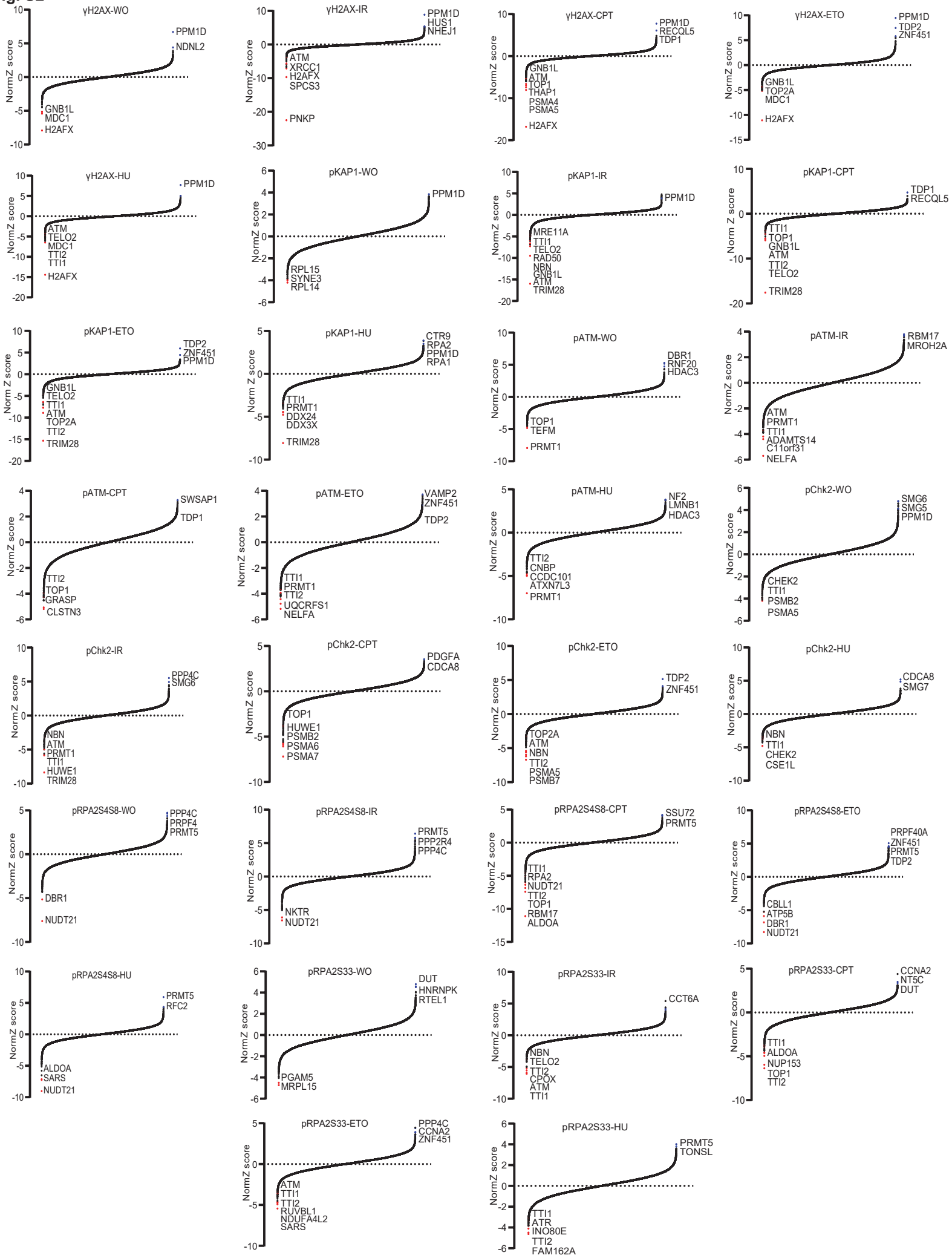
γH2AX-WO
PPM1D
NDNL2
GNB1L
MDC1
H2AFX
γH2AX-IR
PPM1D
HUS1
NHEJ1
ATM
XRCC1
H2AFX
SPCS3
PNKP
γH2AX-CPT
PPM1D
RECQL5
TDP1
GNB1L
ATM
TOP1
THAP1
PSMA4
PSMA5
H2AFX
γH2AX-ETO
PPM1D
TDP2
ZNF451
GNB1L
TOP2A
MDC1
H2AFX
γH2AX-HU
PPM1D
ATM
TELO2
MDC1
TTI2
TTI1
H2AFX
pKAP1-WO
PPM1D
RPL15
SYNE3
RPL14
pKAP1-IR
PPM1D
MRE11A
TTI1
TELO2
RAD50
NBN
GNB1L
ATM
TRIM28
pKAP1-CPT
TDP1
RECQL5
TTI1
TOP1
GNB1L
ATM
TTI2
TELO2
TRIM28
pKAP1-ETO
TDP2
ZNF451
PPM1D
GNB1L
TELO2
TTI1
ATM
TOP2A
TTI2
TRIM28
pKAP1-HU
CTR9
RPA2
PPM1D
RPA1
TTI1
PRMT1
DDX24
DDX3X
TRIM28
pATM-WO
DBR1
RNF20
HDAC3
TOP1
TEFM
PRMT1
pATM-IR
RBM17
MROH2A
ATM
PRMT1
TTI1
ADAMTS14
C11orf31
NELFA
pATM-CPT
SWSAP1
TDP1
TTI2
TOP1
GRASP
CLSTN3
pATM-ETO
VAMP2
ZNF451
TDP2
TTI1
PRMT1
TTI2
UQCRFS1
NELFA
pATM-HU
NF2
LMNB1
HDAC3
TTI2
CNBP
CCDC101
ATXN7L3
PRMT1
pChk2-WO
SMG6
SMG5
PPM1D
CHEK2
TTI1
PSMB2
PSMA5
pChk2-IR
PPP4C
SMG6
NBN
ATM
PRMT1
TTI1
HUWE1
TRIM28
pChk2-CPT
PDGFA
CDCA8
TOP1
HUWE1
PSMB2
PSMA6
PSMA7
pChk2-ETO
TDP2
ZNF451
TOP2A
ATM
NBN
TTI2
PSMA5
PSMB7
pChk2-HU
CDCA8
SMG7
NBN
TTI1
CHEK2
CSE1L
pRPA2S4S8-WO
PPP4C
PRPF4
PRMT5
DBR1
NUDT21
pRPA2S4S8-IR
PRMT5
PPP2R4
PPP4C
NKTR
NUDT21
pRPA2S4S8-CPT
SSU72
PRMT5
TTI1
RPA2
NUDT21
TTI2
TOP1
RBM17
ALDOA
pRPA2S4S8-ETO
PRPF40A
ZNF451
PRMT5
TDP2
CBLL1
ATP5B
DBR1
NUDT21
pRPA2S4S8-HU
PRMT5
RFC2
ALDOA
SARS
NUDT21
pRPA2S33-WO
DUT
HNRNPK
RTEL1
PGAM5
MRPL15
pRPA2S33-IR
CCT6A
NBN
TELO2
TTI2
CPOX
ATM
TTI1
pRPA2S33-CPT
CCNA2
NT5C
DUT
TTI1
ALDOA
NUP153
TOP1
TTI2
pRPA2S33-ETO
PPP4C
CCNA2
ZNF451
ATM
TTI1
TTI2
RUVBL1
NDUFA4L2
SARS
pRPA2S33-HU
PRMT5
TONSL
TTI1
ATR
INO80E
TTI2
FAM162A

Fig. S3

A

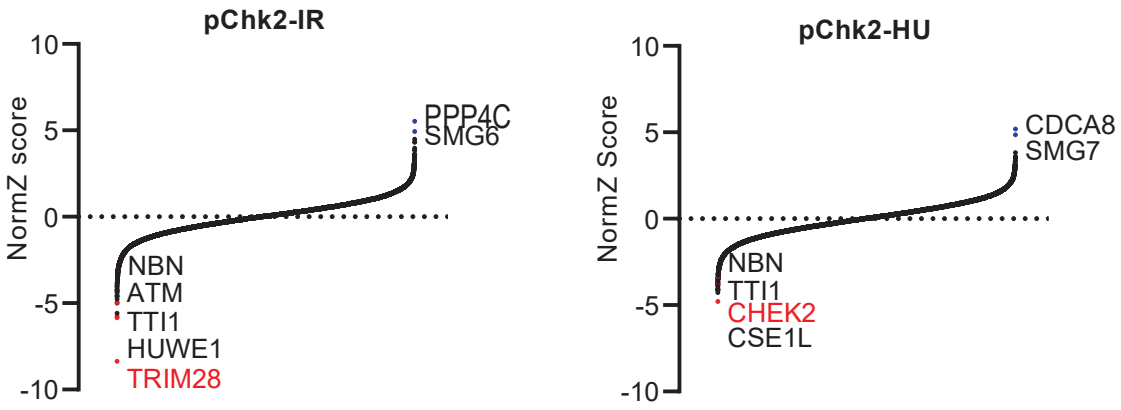
pChk2-IR
NormZ score
10
5
0
-5
-10
PPP4C
SMG6
NBN
ATM
TTI1
HUWE1
TRIM28
pChk2-HU
NormZ Score
CDCA8
SMG7
NBN
TTI1
CHEK2
CSE1L

B

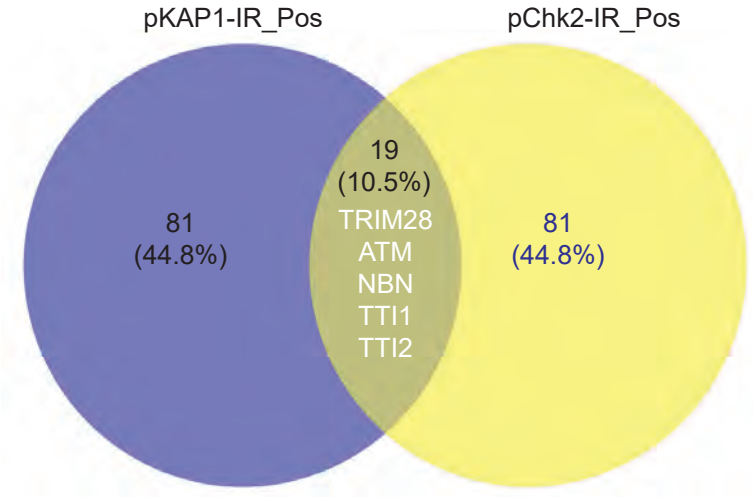
pKAP1-IR_Pos
pChk2-IR_Pos
81
(44.8%)
19
(10.5%)
TRIM28
ATM
NBN
TTI1
TTI2
81
(44.8%)

C

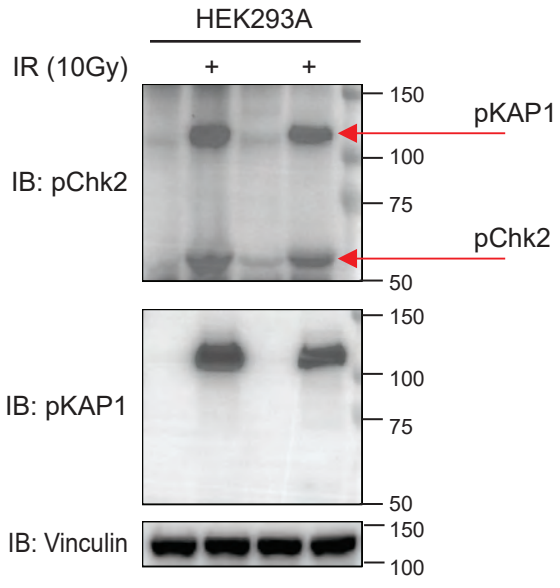
HEK293A
IR (10Gy)
+
+
IB: pChk2
150
100
75
50
pKAP1
pChk2
IB: pKAP1
150
100
75
50
IB: Vinculin
150
100

Fig. S4

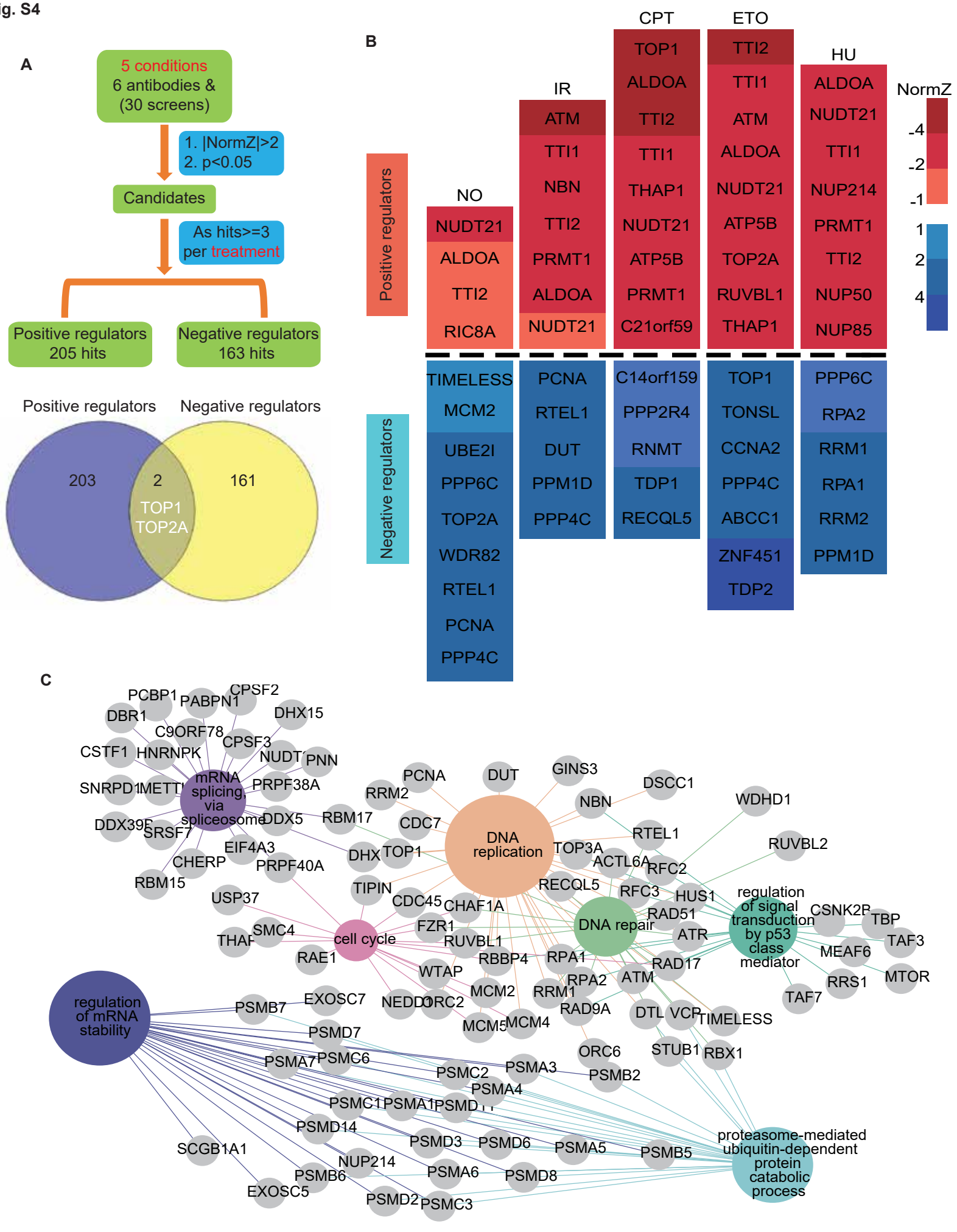
A
5 conditions
6 antibodies &
(30 screens)
1. |NormZ|>2
2. p<0.05
Candidates
As hits>=3
per treatment
Positive regulators
205 hits
Negative regulators
163 hits
Positive regulators
Negative regulators
203
2
TOP1
TOP2A
161
B
NO
IR
CPT
ETO
HU
Positive regulators
NUDT21
ALDOA
TTI2
RIC8A
ATM
TTI1
NBN
TTI2
PRMT1
ALDOA
NUDT21
TOP1
ALDOA
TTI2
TTI1
THAP1
NUDT21
ATP5B
PRMT1
C21orf59
TTI2
TTI1
ATM
ALDOA
NUDT21
ATP5B
TOP2A
RUVBL1
THAP1
ALDOA
NUDT21
TTI1
NUP214
PRMT1
TTI2
NUP50
NUP85
NormZ
-4
-2
-1
1
2
4
Negative regulators
TIMELESS
MCM2
UBE2I
PPP6C
TOP2A
WDR82
RTEL1
PCNA
PPP4C
PCNA
RTEL1
DUT
PPM1D
PPP4C
C14orf159
PPP2R4
RNMT
TDP1
RECQL5
TOP1
TONSL
CCNA2
PPP4C
ABCC1
ZNF451
TDP2
PPP6C
RPA2
RRM1
RPA1
RRM2
PPM1D
C
PCBP1
PABPN1
CPSF2
DBR1
DHX15
C9ORF78
CPSF3
CSTF1
HNRNPK
NUDT
PNN
SNRPD1
METTL
PRPF38A
DDX39B
SRSF7
DDX5
RBM17
EIF4A3
CHERP
PRPF40A
RBM15
mRNA splicing, via spliceosome
PCNA
DUT
GINS3
RRM2
CDC7
DHX
TOP1
DNA replication
DSCC1
NBN
WDHD1
RTEL1
TOP3A
ACTL6A
RFC2
RUVBL2
RECQL5
RFC3
HUS1
RAD51
ATR
TIPIN
CDC45
CHAF1A
USP37
FZR1
RUVBL1
RBBP4
RPA1
RAD17
RPA2
ATM
WTAP
MCM2
RRM1
RAD9A
DTL
VCP
TIMELESS
MCM5
MCM4
ORC2
NEDD
ORC6
STUB1
RBX1
PSMB2
THAP
SMC4
RAE1
cell cycle
DNA repair
regulation of signal transduction by p53 class mediator
CSNK2B
TBP
TAF3
MEAF6
RRS1
MTOR
TAF7
regulation of mRNA stability
PSMB7
EXOSC7
PSMD7
PSMA7
PSMC6
PSMC2
PSMA3
PSMA4
PSMC1
PSMA1
PSMD11
PSMD14
PSMD3
PSMD6
PSMA5
PSMB5
SCGB1A1
NUP214
PSMB6
PSMA6
PSMD8
EXOSC5
PSMD2
PSMC3
proteasome-mediated ubiquitin-dependent protein catabolic process

Fig. S5

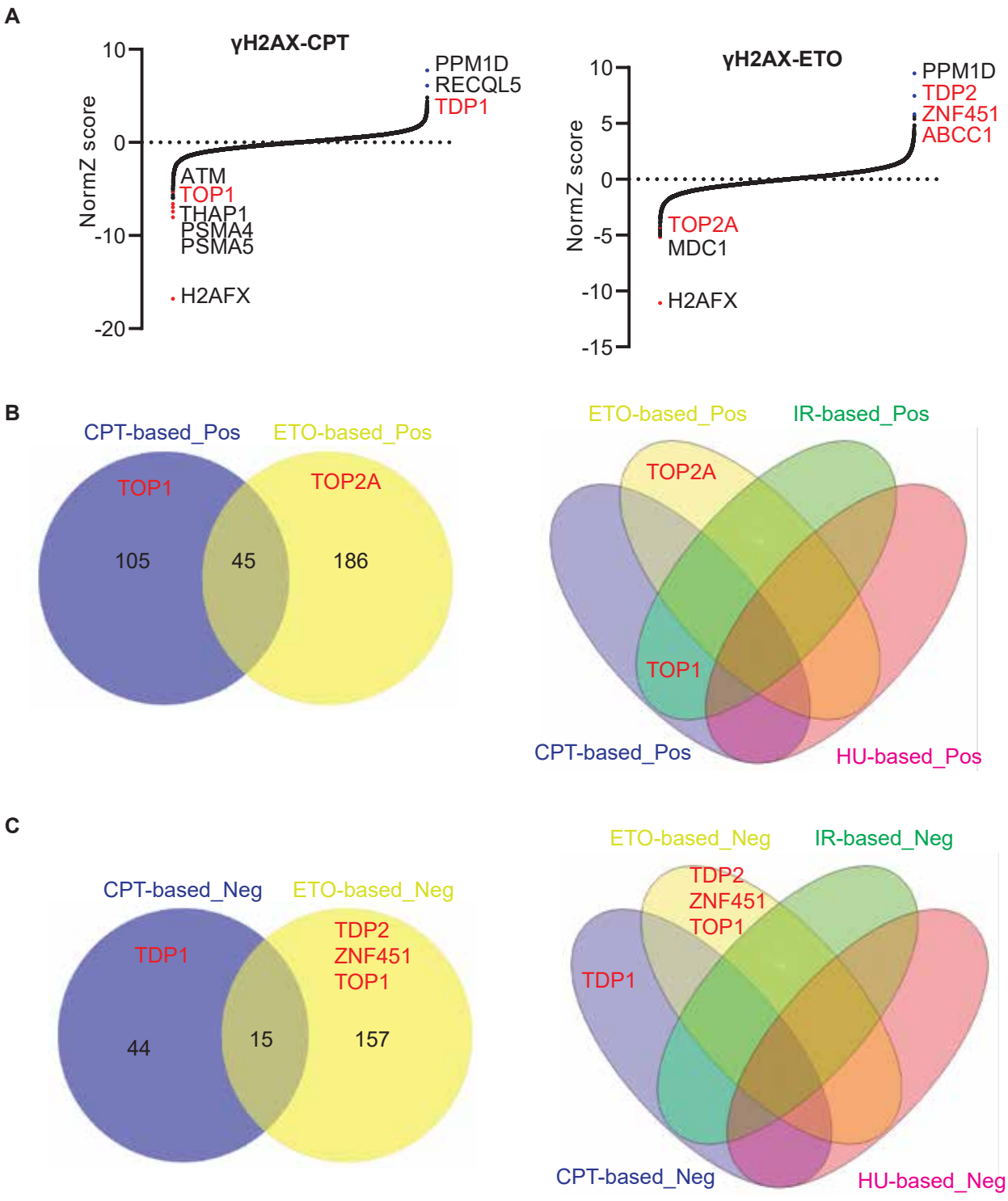
A
γH2AX-CPT
NormZ score
PPM1D
RECQL5
TDP1
ATM
TOP1
THAP1
PSMA4
PSMA5
H2AFX
γH2AX-ETO
PPM1D
TDP2
ZNF451
ABCC1
TOP2A
MDC1
H2AFX
B
CPT-based_Pos
ETO-based_Pos
TOP1
TOP2A
105
45
186
ETO-based_Pos
IR-based_Pos
TOP2A
TOP1
CPT-based_Pos
HU-based_Pos
C
CPT-based_Neg
ETO-based_Neg
TDP1
TDP2
ZNF451
TOP1
44
15
157
ETO-based_Neg
IR-based_Neg
TDP2
ZNF451
TOP1
TDP1
CPT-based_Neg
HU-based_Neg
D
NO
IR
CPT
ETO
HU
pATM
pChk2
pKAP1
γH2AX
pRPA2-S4/S8
pRPA2-S33
TOP1
TDP1
RECQL5
TOP2A
TDP2
ZNF451
6
4
2
0
-2
-4
-6

Fig. S6

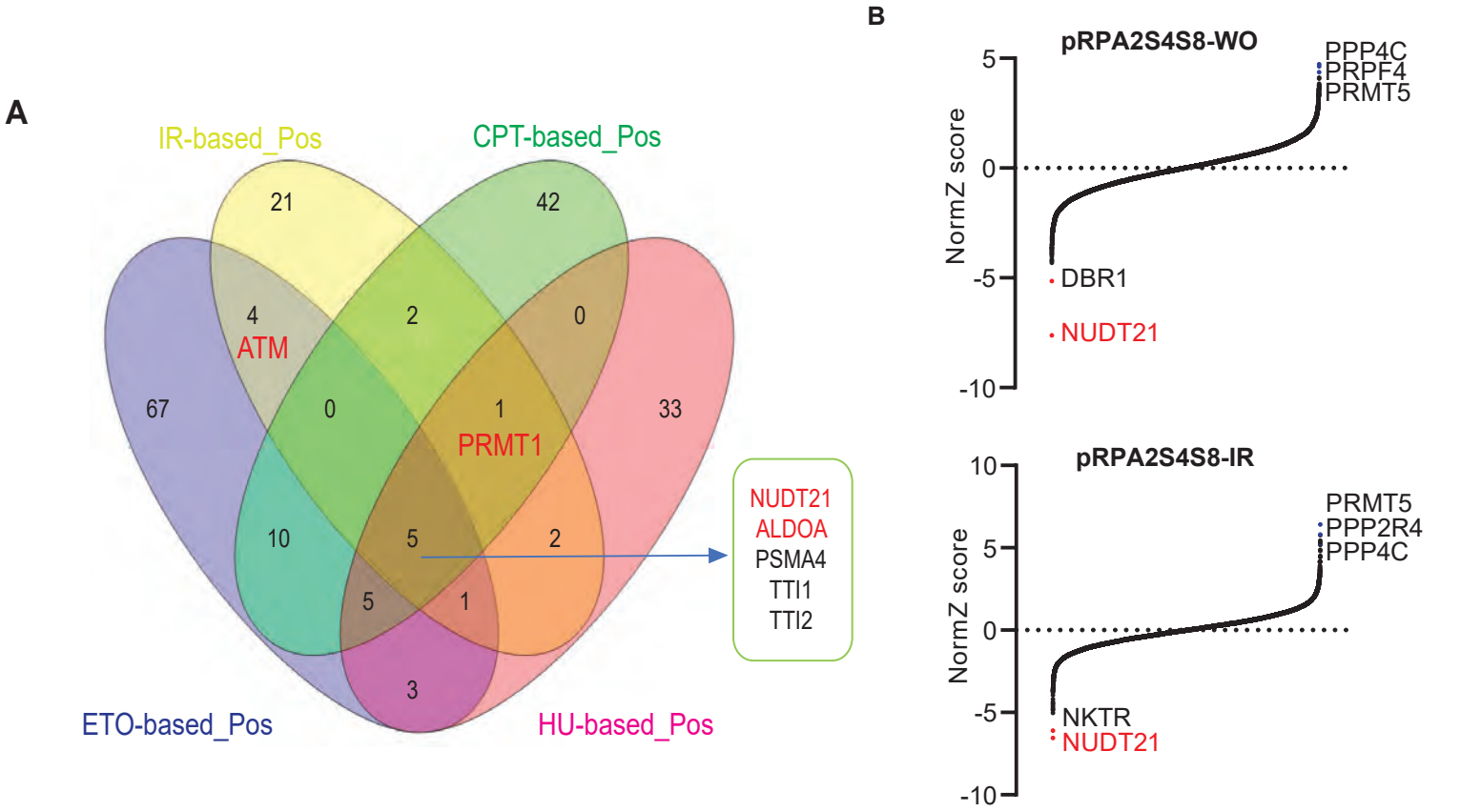
A
IR-based_Pos
CPT-based_Pos
ETO-based_Pos
HU-based_Pos
21
42
4
ATM
2
0
67
0
1
PRMT1
33
10
5
2
5
1
3
NUDT21
ALDOA
PSMA4
TTI1
TTI2
B
pRPA2S4S8-WO
NormZ score
5
0
-5
-10
PPP4C
PRPF4
PRMT5
DBR1
NUDT21
pRPA2S4S8-IR
NormZ score
10
5
0
-5
-10
PRMT5
PPP2R4
PPP4C
NKTR
NUDT21

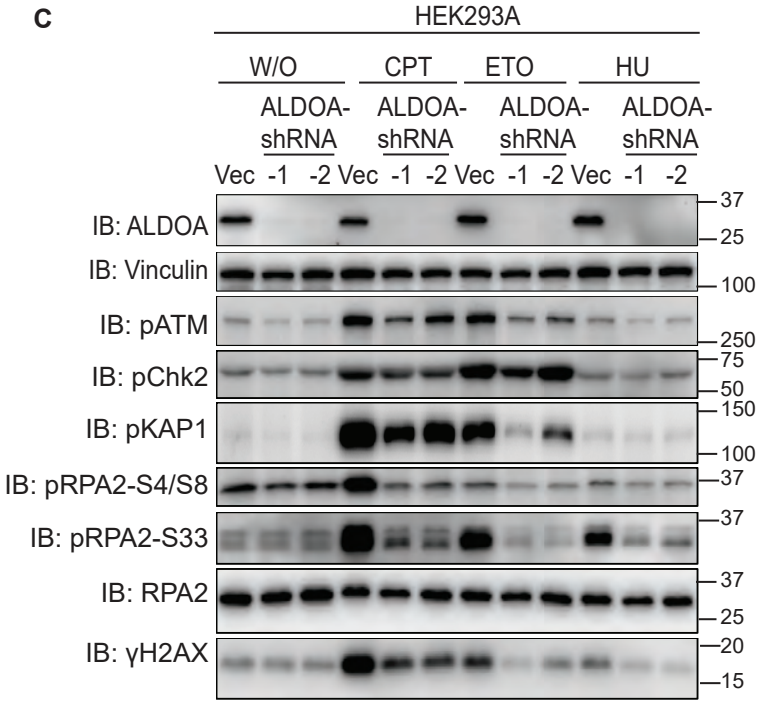
C
HEK293A
W/O
CPT
ETO
HU
ALDOA-shRNA
Vec -1 -2 Vec -1 -2 Vec -1 -2 Vec -1 -2
IB: ALDOA
IB: Vinculin
IB: pATM
IB: pChk2
IB: pKAP1
IB: pRPA2-S4/S8
IB: pRPA2-S33
IB: RPA2
IB: γH2AX
37
25
100
250
75
50
150
100
37
37
37
25
20
15

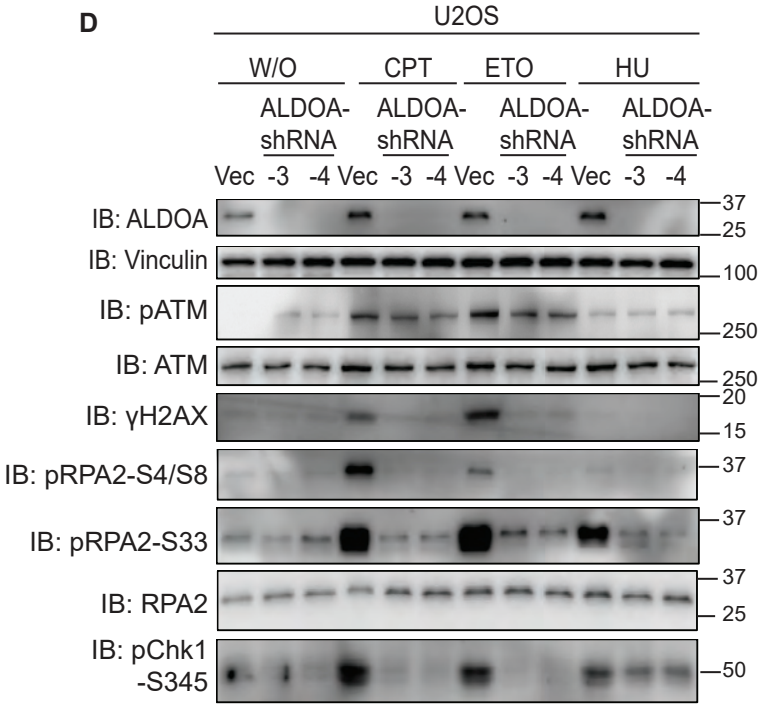
D
U2OS
W/O
CPT
ETO
HU
ALDOA-shRNA
Vec -3 -4 Vec -3 -4 Vec -3 -4 Vec -3 -4
IB: ALDOA
IB: Vinculin
IB: pATM
IB: ATM
IB: γH2AX
IB: pRPA2-S4/S8
IB: pRPA2-S33
IB: RPA2
IB: pChk1 -S345
37
25
100
250
250
20
15
37
37
37
25
50

Fig. S7

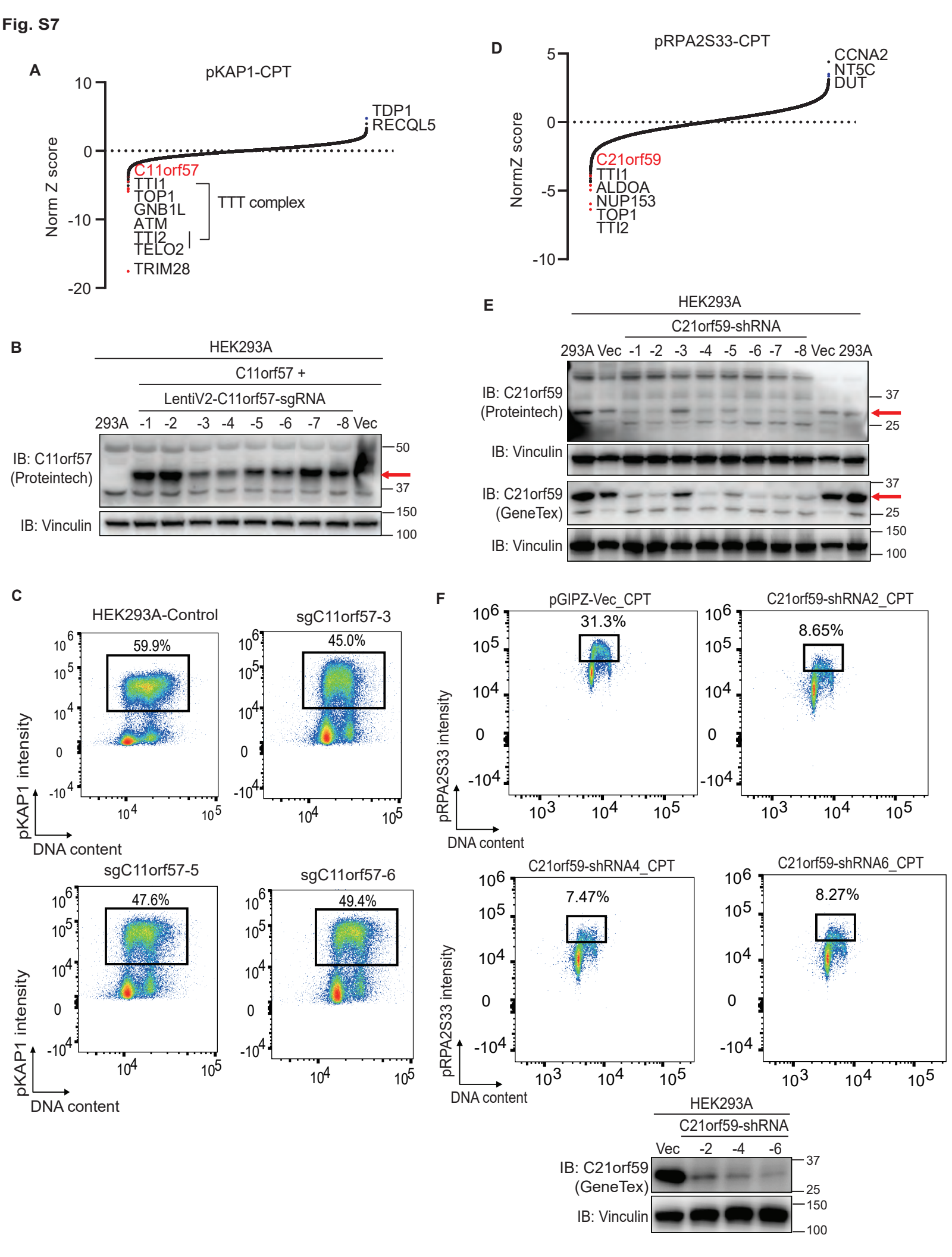
A
pKAP1-CPT
Norm Z score
10
0
-10
-20
TDP1
RECQL5
C11orf57
TTI1
TOP1
GNB1L
ATM
TTI2
TELO2
TTT complex
TRIM28
D
pRPA2S33-CPT
NormZ score
5
0
-5
-10
CCNA2
NT5C
DUT
C21orf59
TTI1
ALDOA
NUP153
TOP1
TTI2
B
HEK293A
C11orf57 +
LentiV2-C11orf57-sgRNA
293A -1 -2 -3 -4 -5 -6 -7 -8 Vec
IB: C11orf57 (Proteintech)
IB: Vinculin
50
37
150
100
E
HEK293A
C21orf59-shRNA
293A Vec -1 -2 -3 -4 -5 -6 -7 -8 Vec 293A
IB: C21orf59 (Proteintech)
IB: Vinculin
IB: C21orf59 (GeneTex)
IB: Vinculin
37
25
150
100
C
HEK293A-Control
59.9%
sgC11orf57-3
45.0%
sgC11orf57-5
47.6%
sgC11orf57-6
49.4%
pKAP1 intensity
DNA content
F
pGIPZ-Vec_CPT
31.3%
C21orf59-shRNA2_CPT
8.65%
C21orf59-shRNA4_CPT
7.47%
C21orf59-shRNA6_CPT
8.27%
pRPA2S33 intensity
DNA content
HEK293A
C21orf59-shRNA
Vec -2 -4 -6
IB: C21orf59 (GeneTex)
IB: Vinculin
37
25
150
100

Fig. S8

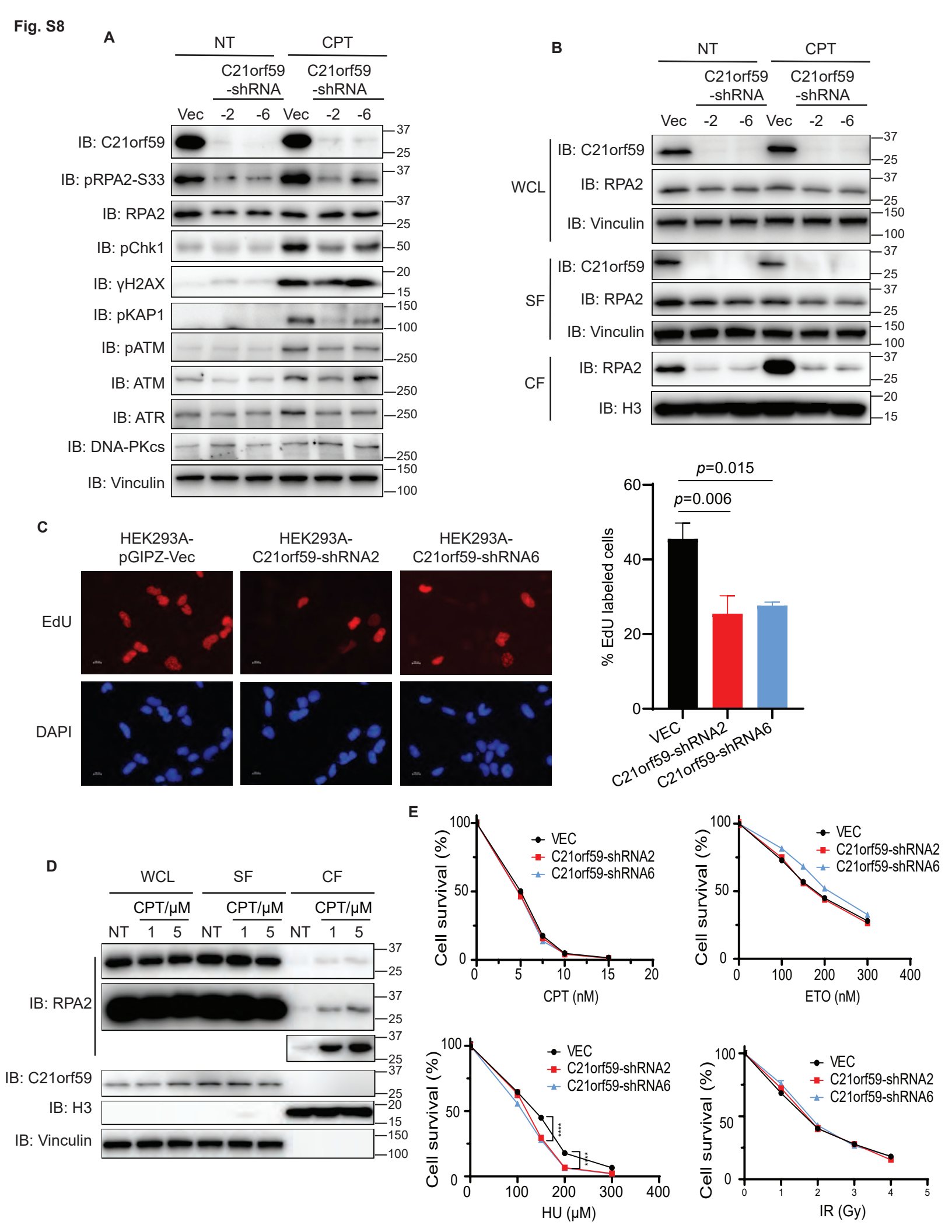
A
NT
CPT
C21orf59 -shRNA
C21orf59 -shRNA
Vec -2 -6 Vec -2 -6
IB: C21orf59
IB: pRPA2-S33
IB: RPA2
IB: pChk1
IB: γH2AX
IB: pKAP1
IB: pATM
IB: ATM
IB: ATR
IB: DNA-PKcs
IB: Vinculin
B
NT
CPT
C21orf59 -shRNA
C21orf59 -shRNA
Vec -2 -6 Vec -2 -6
WCL
SF
CF
IB: C21orf59
IB: RPA2
IB: Vinculin
IB: H3
C
HEK293A-pGIPZ-Vec
HEK293A-C21orf59-shRNA2
HEK293A-C21orf59-shRNA6
EdU
DAPI
p=0.015
p=0.006
% EdU labeled cells
VEC
C21orf59-shRNA2
C21orf59-shRNA6
D
WCL
SF
CF
CPT/μM
NT 1 5 NT 1 5 NT 1 5
IB: RPA2
IB: C21orf59
IB: H3
IB: Vinculin
E
Cell survival (%)
CPT (nM)
ETO (nM)
HU (μM)
IR (Gy)
VEC
C21orf59-shRNA2
C21orf59-shRNA6

Fig. S9

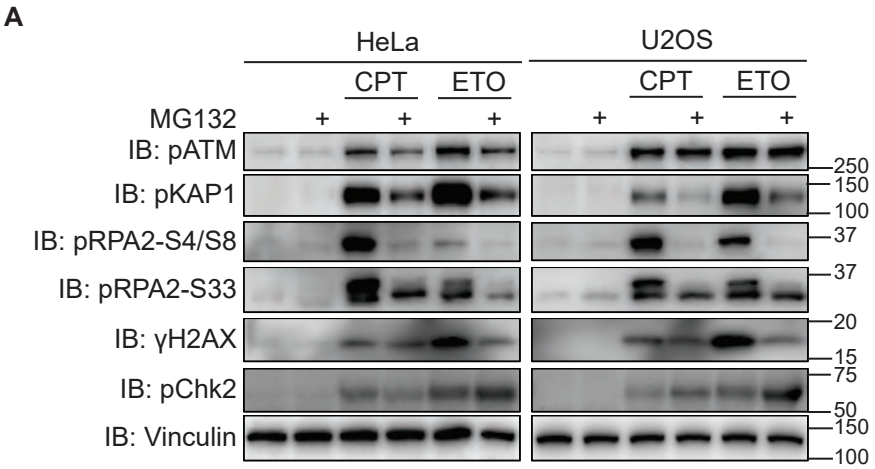
A
HeLa
U2OS
CPT
ETO
CPT
ETO
MG132
+ + + + + +
IB: pATM
IB: pKAP1
IB: pRPA2-S4/S8
IB: pRPA2-S33
IB: γH2AX
IB: pChk2
IB: Vinculin
250
150
100
37
37
20
15
75
50
150
100

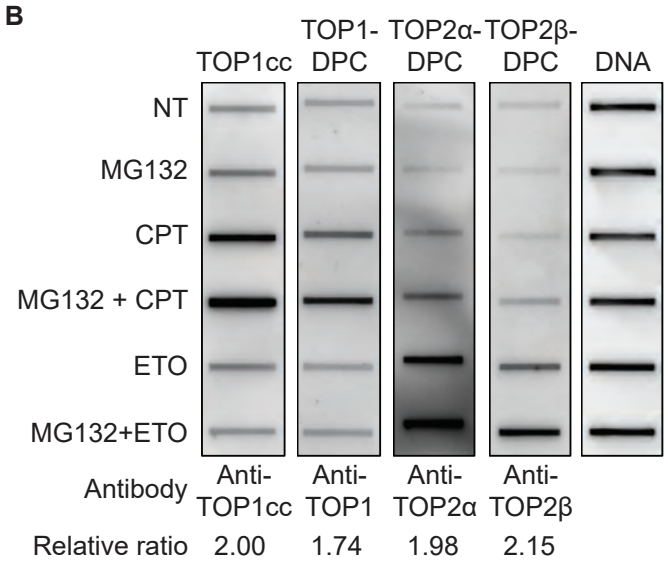
B
TOP1cc
TOP1-DPC
TOP2α-DPC
TOP2β-DPC
DNA
NT
MG132
CPT
MG132 + CPT
ETO
MG132+ETO
Antibody
Anti-TOP1cc
Anti-TOP1
Anti-TOP2α
Anti-TOP2β
Relative ratio
2.00
1.74
1.98
2.15

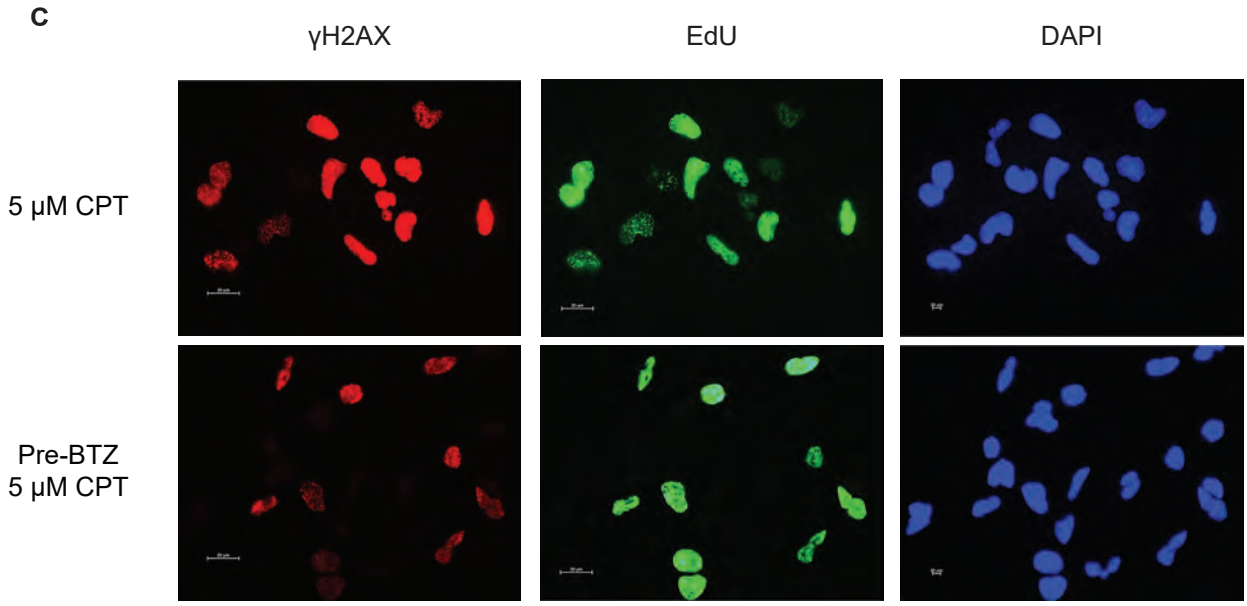
C
γH2AX
EdU
DAPI
5 μM CPT
Pre-BTZ
5 μM CPT

Fig. S10

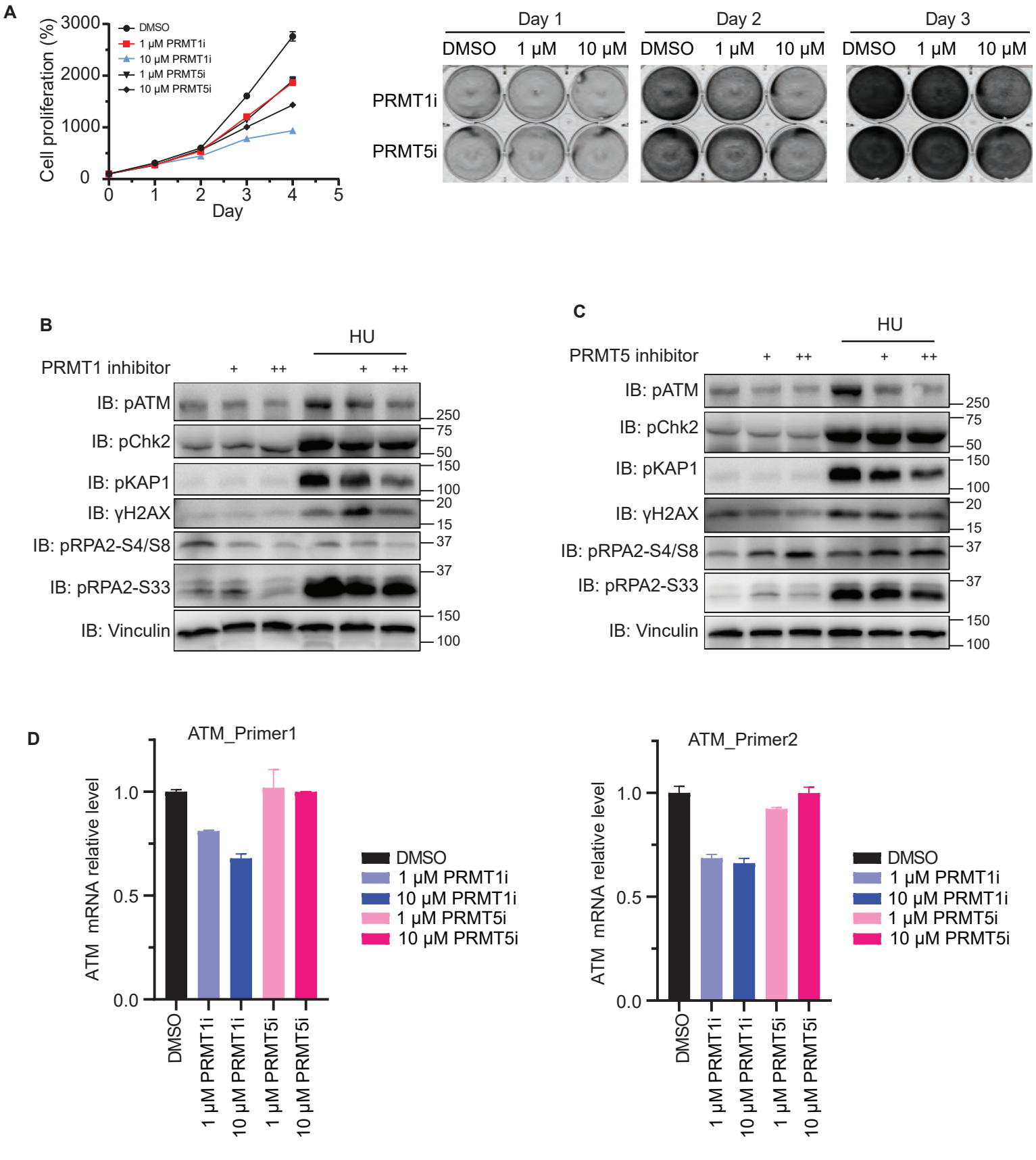
A
Cell proliferation (%)
3000
2000
1000
0
0 1 2 3 4 5
Day
DMSO
1 μM PRMT1i
10 μM PRMT1i
1 μM PRMT5i
10 μM PRMT5i
Day 1
Day 2
Day 3
DMSO 1 μM 10 μM
PRMT1i
PRMT5i
B
HU
PRMT1 inhibitor + ++ + ++
IB: pATM
IB: pChk2
IB: pKAP1
IB: γH2AX
IB: pRPA2-S4/S8
IB: pRPA2-S33
IB: Vinculin
250
75
50
150
100
20
15
37
37
150
100
C
HU
PRMT5 inhibitor + ++ + ++
IB: pATM
IB: pChk2
IB: pKAP1
IB: γH2AX
IB: pRPA2-S4/S8
IB: pRPA2-S33
IB: Vinculin
250
75
50
150
100
20
15
37
37
150
100
D
ATM_Primer1
ATM mRNA relative level
1.0
0.5
0.0
DMSO
1 μM PRMT1i
10 μM PRMT1i
1 μM PRMT5i
10 μM PRMT5i
ATM_Primer2
ATM mRNA relative level
1.0
0.5
0.0
DMSO
1 μM PRMT1i
10 μM PRMT1i
1 μM PRMT5i
10 μM PRMT5i

Fig. S11

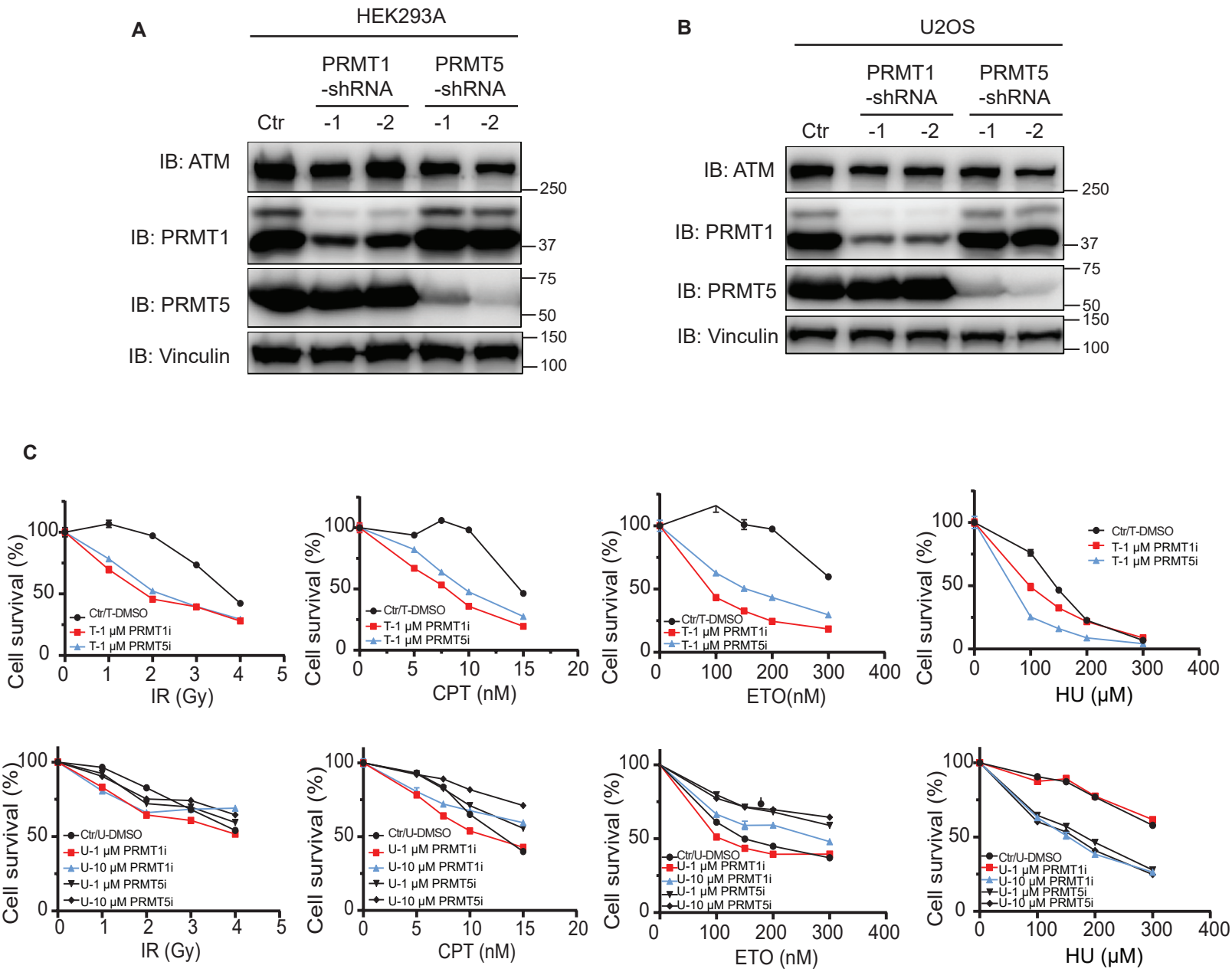
A
HEK293A
PRMT1 -shRNA
PRMT5 -shRNA
Ctr
-1
-2
-1
-2
IB: ATM
IB: PRMT1
IB: PRMT5
IB: Vinculin
250
37
75
50
150
100
B
U2OS
PRMT1 -shRNA
PRMT5 -shRNA
Ctr
-1
-2
-1
-2
IB: ATM
IB: PRMT1
IB: PRMT5
IB: Vinculin
250
37
75
50
150
100
C
Cell survival (%)
Ctr/T-DMSO
T-1 μM PRMT1i
T-1 μM PRMT5i
IR (Gy)
CPT (nM)
ETO(nM)
HU (μM)
Ctr/U-DMSO
U-1 μM PRMT1i
U-10 μM PRMT1i
U-1 μM PRMT5i
U-10 μM PRMT5i
IR (Gy)
CPT (nM)
ETO (nM)
HU (μM)

Fig. S12

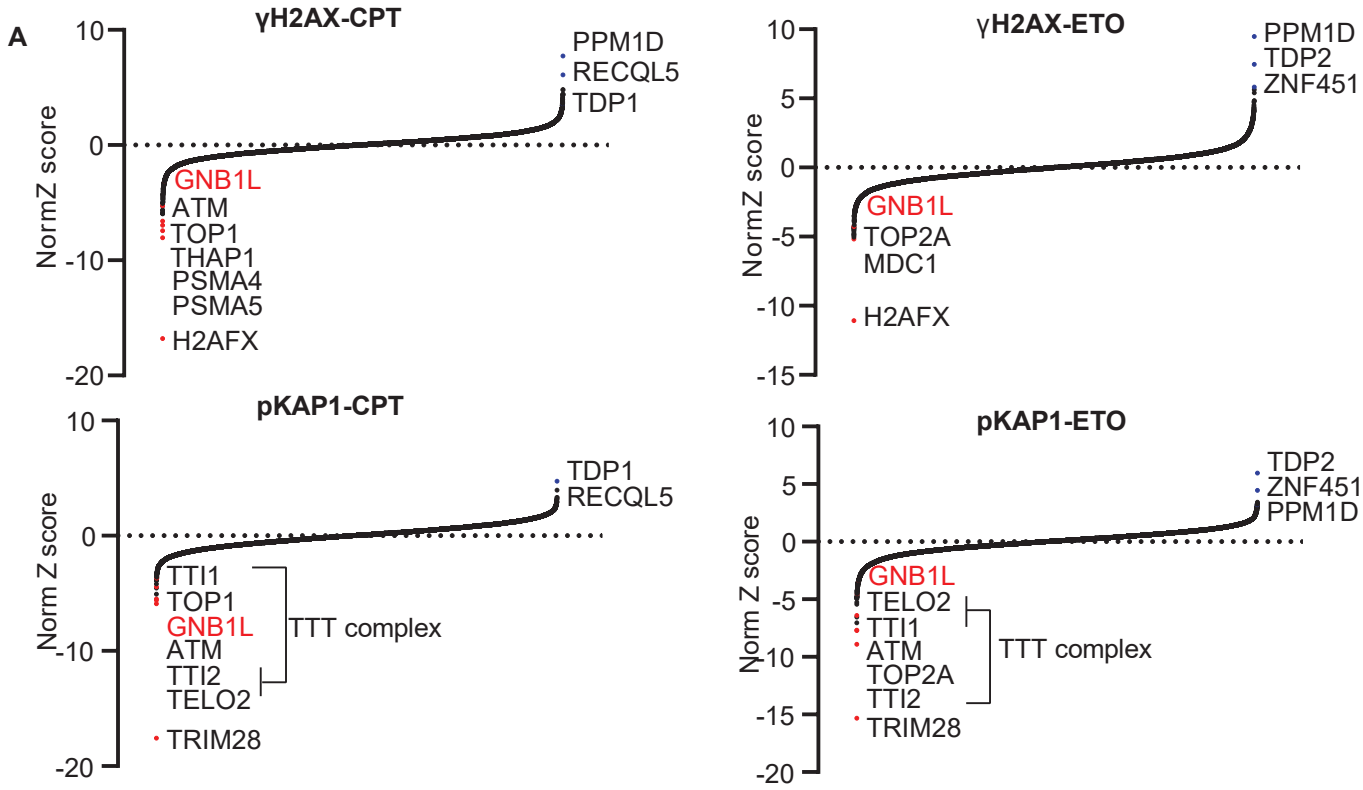
A
γH2AX-CPT
NormZ score
PPM1D
RECQL5
TDP1
GNB1L
ATM
TOP1
THAP1
PSMA4
PSMA5
H2AFX
γH2AX-ETO
PPM1D
TDP2
ZNF451
GNB1L
TOP2A
MDC1
H2AFX
pKAP1-CPT
Norm Z score
TDP1
RECQL5
TTI1
TOP1
GNB1L
ATM
TTI2
TELO2
TTT complex
TRIM28
pKAP1-ETO
TDP2
ZNF451
PPM1D
GNB1L
TELO2
TTI1
ATM
TOP2A
TTI2
TTT complex
TRIM28

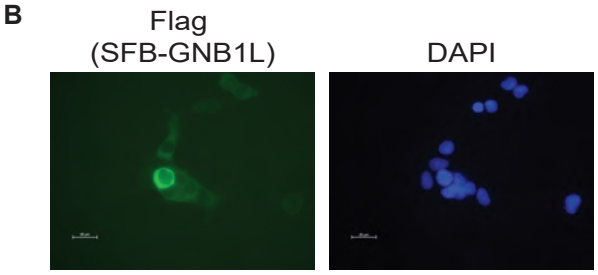
B
Flag
(SFB-GNB1L)
DAPI

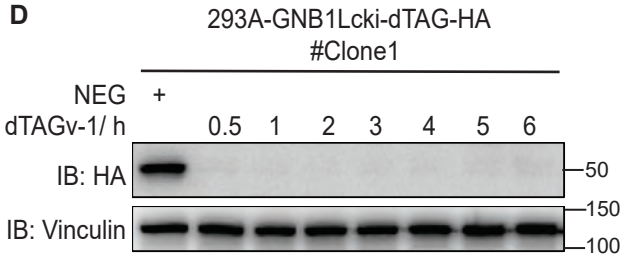
D
293A-GNB1Lcki-dTAG-HA
#Clone1
NEG
+
dTAGv-1/ h
0.5 1 2 3 4 5 6
IB: HA
IB: Vinculin
50
150
100

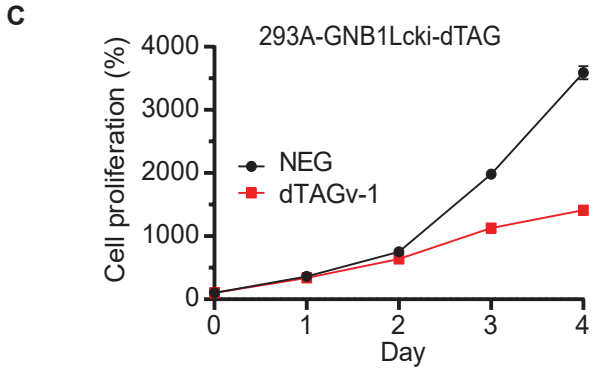
C
293A-GNB1Lcki-dTAG
Cell proliferation (%)
NEG
dTAGv-1
Day

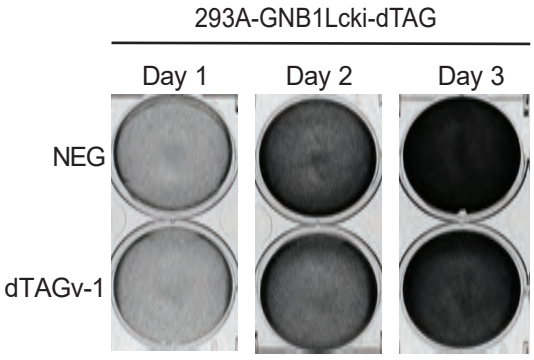
293A-GNB1Lcki-dTAG
Day 1
Day 2
Day 3
NEG
dTAGv-1

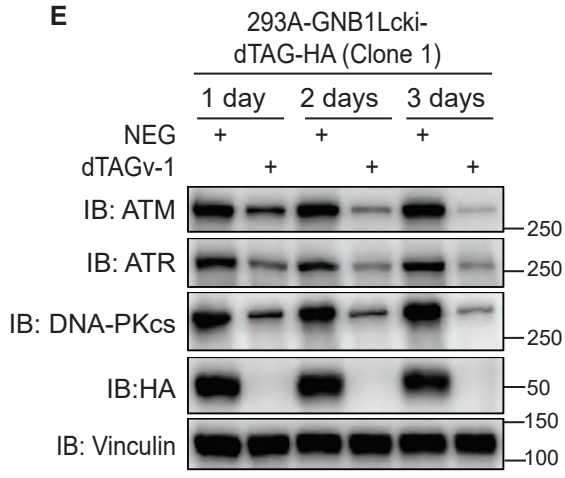
E
293A-GNB1Lcki-
dTAG-HA (Clone 1)
1 day
2 days
3 days
NEG
dTAGv-1
IB: ATM
IB: ATR
IB: DNA-PKcs
IB:HA
IB: Vinculin
250
250
250
50
150
100

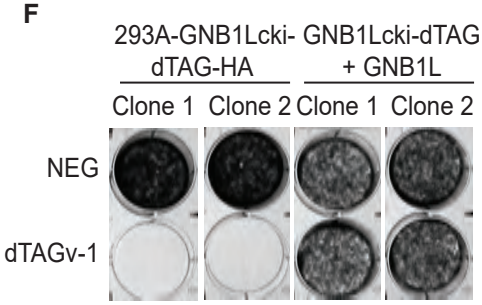
F
293A-GNB1Lcki-
dTAG-HA
GNB1Lcki-dTAG
+ GNB1L
Clone 1
Clone 2
Clone 1
Clone 2
NEG
dTAGv-1

Fig. S13

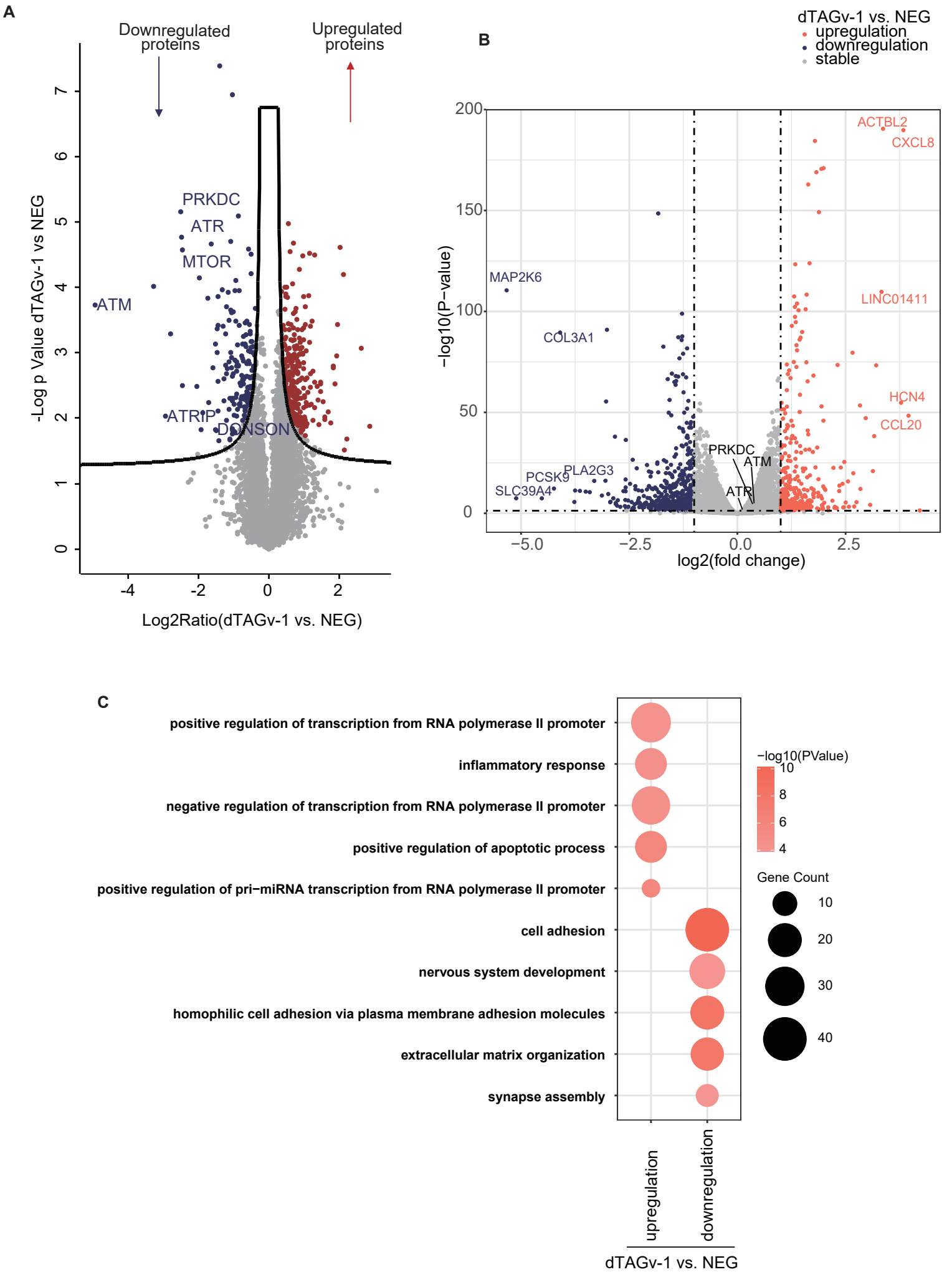
A
Downregulated proteins
Upregulated proteins
PRKDC
ATR
MTOR
ATM
ATRIP
DONSON
-Log p Value dTAGv-1 vs NEG
Log2Ratio(dTAGv-1 vs. NEG)
B
dTAGv-1 vs. NEG
upregulation
downregulation
stable
ACTBL2
CXCL8
LINC01411
HCN4
CCL20
MAP2K6
COL3A1
PRKDC
ATM
ATR
PLA2G3
PCSK9
SLC39A4
−log10(P−value)
log2(fold change)
C
positive regulation of transcription from RNA polymerase II promoter
inflammatory response
negative regulation of transcription from RNA polymerase II promoter
positive regulation of apoptotic process
positive regulation of pri−miRNA transcription from RNA polymerase II promoter
cell adhesion
nervous system development
homophilic cell adhesion via plasma membrane adhesion molecules
extracellular matrix organization
synapse assembly
−log10(PValue)
Gene Count
upregulation
downregulation
dTAGv-1 vs. NEG

Fig. S14

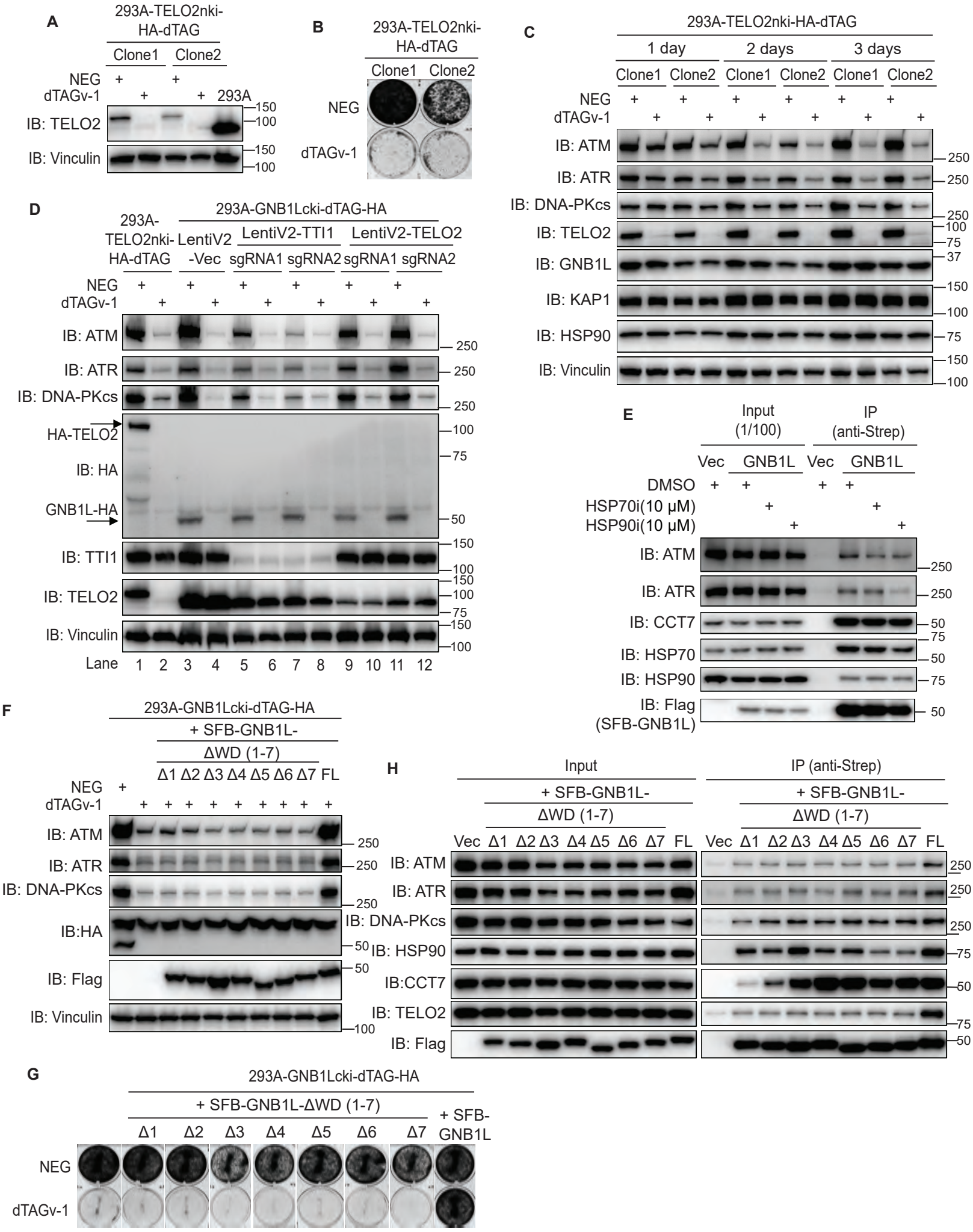
A
293A-TELO2nki-HA-dTAG
Clone1
Clone2
NEG
dTAGv-1
293A
IB: TELO2
IB: Vinculin
150
100
B
293A-TELO2nki-HA-dTAG
Clone1
Clone2
NEG
dTAGv-1
C
293A-TELO2nki-HA-dTAG
1 day
2 days
3 days
Clone1
Clone2
NEG
dTAGv-1
IB: ATM
IB: ATR
IB: DNA-PKcs
IB: TELO2
IB: GNB1L
IB: KAP1
IB: HSP90
IB: Vinculin
250
100
75
37
150
D
293A-TELO2nki-HA-dTAG
293A-GNB1Lcki-dTAG-HA
LentiV2-Vec
LentiV2-TTI1
LentiV2-TELO2
sgRNA1
sgRNA2
NEG
dTAGv-1
IB: ATM
IB: ATR
IB: DNA-PKcs
HA-TELO2
IB: HA
GNB1L-HA
IB: TTI1
IB: TELO2
IB: Vinculin
250
100
75
50
150
Lane 1 2 3 4 5 6 7 8 9 10 11 12
E
Input (1/100)
IP (anti-Strep)
Vec
GNB1L
DMSO
HSP70i(10 μM)
HSP90i(10 μM)
IB: ATM
IB: ATR
IB: CCT7
IB: HSP70
IB: HSP90
IB: Flag (SFB-GNB1L)
250
50
75
F
293A-GNB1Lcki-dTAG-HA
+ SFB-GNB1L-ΔWD (1-7)
Δ1 Δ2 Δ3 Δ4 Δ5 Δ6 Δ7 FL
NEG
dTAGv-1
IB: ATM
IB: ATR
IB: DNA-PKcs
IB:HA
IB: Flag
IB: Vinculin
250
50
100
H
Input
IP (anti-Strep)
+ SFB-GNB1L-ΔWD (1-7)
Vec Δ1 Δ2 Δ3 Δ4 Δ5 Δ6 Δ7 FL
IB: ATM
IB: ATR
IB: DNA-PKcs
IB: HSP90
IB:CCT7
IB: TELO2
IB: Flag
250
75
50
G
293A-GNB1Lcki-dTAG-HA
+ SFB-GNB1L-ΔWD (1-7)
Δ1 Δ2 Δ3 Δ4 Δ5 Δ6 Δ7
+ SFB-GNB1L
NEG
dTAGv-1

Fig. S15

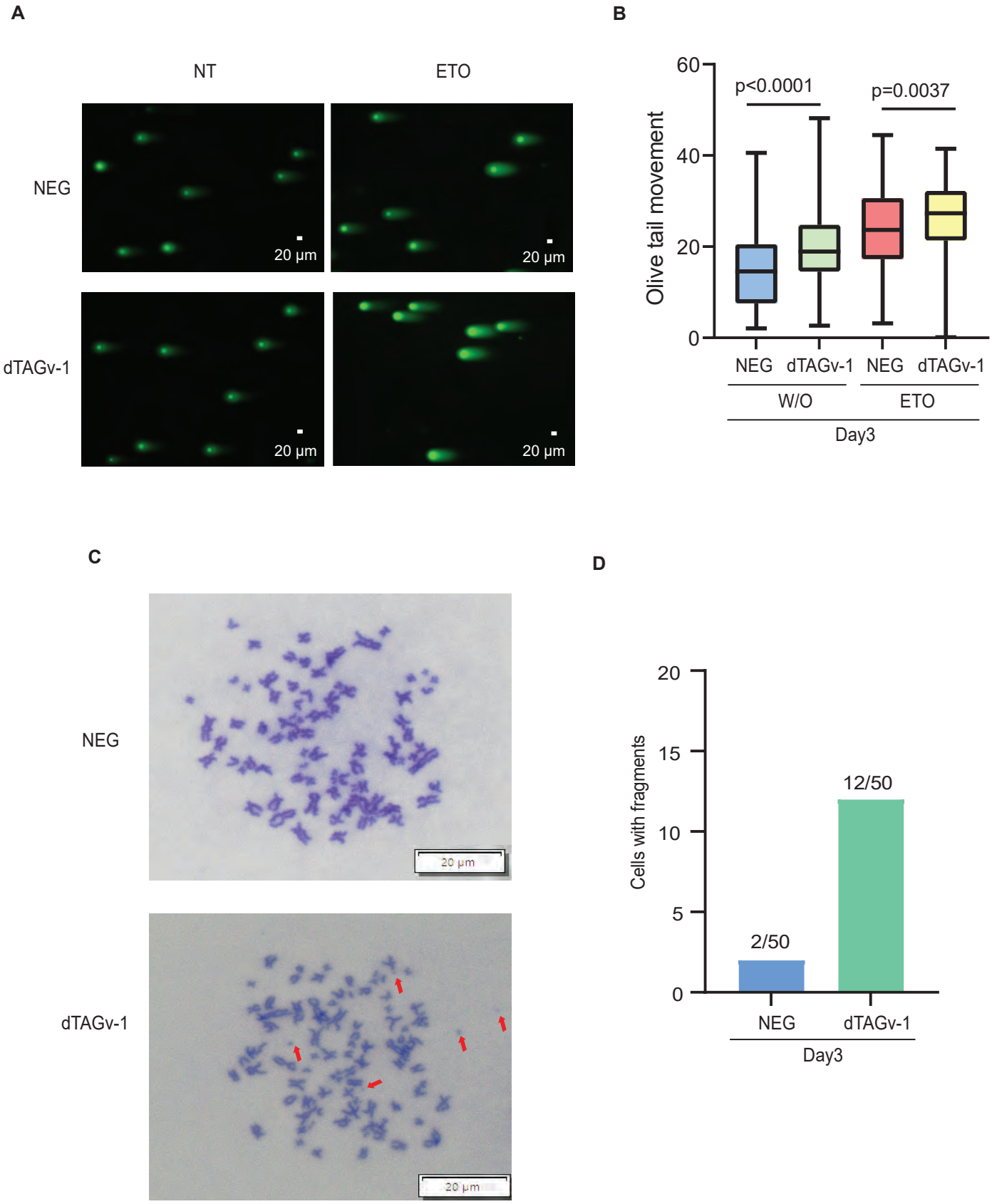
A
NT
ETO
NEG
dTAGv-1
20 µm
B
Olive tail movement
60
40
20
0
p<0.0001
p=0.0037
NEG
dTAGv-1
NEG
dTAGv-1
W/O
ETO
Day3
C
NEG
dTAGv-1
20 µm
D
Cells with fragments
20
15
10
5
0
12/50
2/50
NEG
dTAGv-1
Day3

Fig. S16

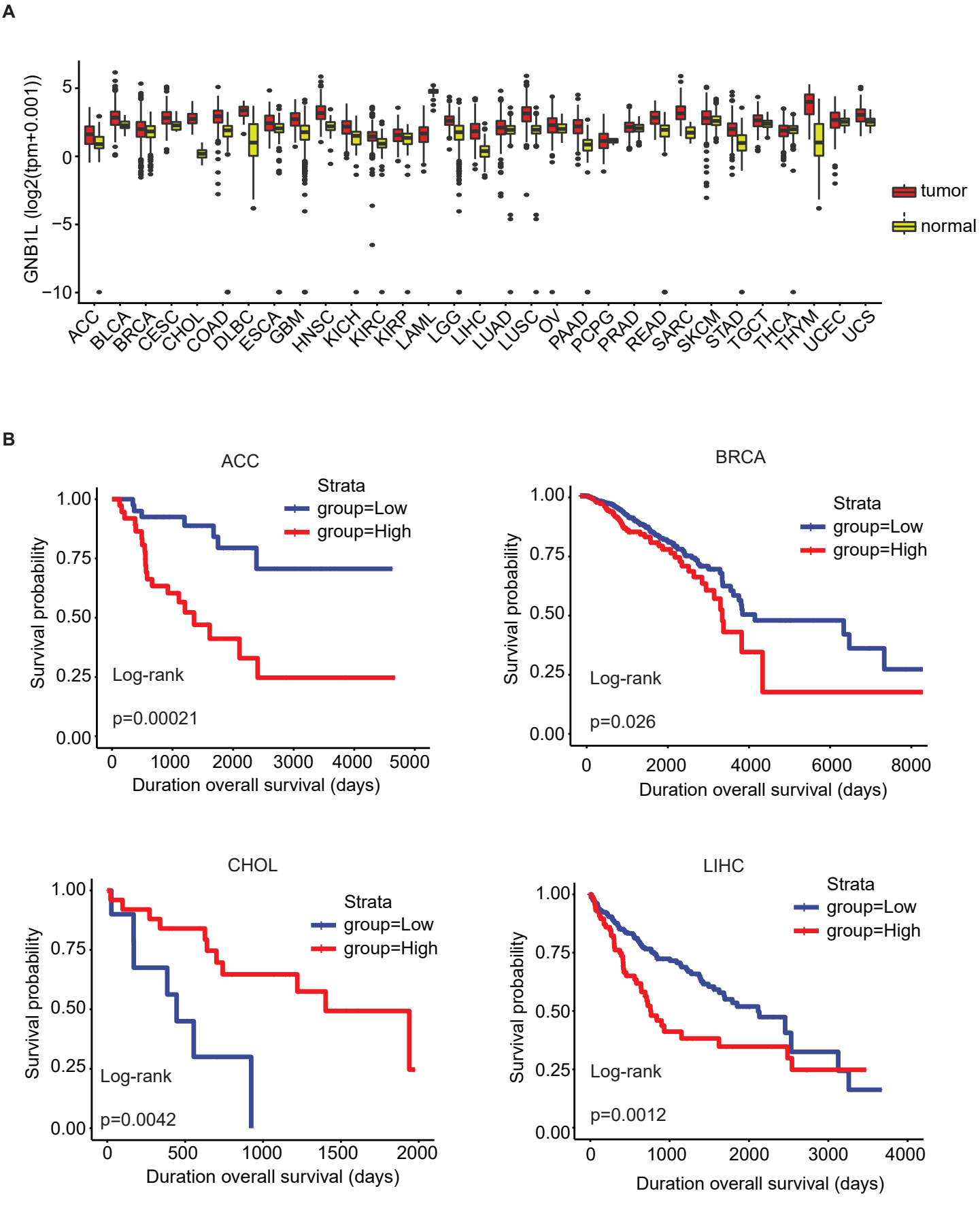
A
GNB1L (log2(tpm+0.001))
5
0
−5
−10
ACC
BLCA
BRCA
CESC
CHOL
COAD
DLBC
ESCA
GBM
HNSC
KICH
KIRC
KIRP
LAML
LGG
LIHC
LUAD
LUSC
OV
PAAD
PCPG
PRAD
READ
SARC
SKCM
STAD
TGCT
THCA
THYM
UCEC
UCS
tumor
normal
B
ACC
Strata
group=Low
group=High
Survival probability
1.00
0.75
0.50
0.25
0.00
Log-rank
p=0.00021
0
1000
2000
3000
4000
5000
Duration overall survival (days)
BRCA
Strata
group=Low
group=High
Survival probability
1.00
0.75
0.50
0.25
0.00
Log-rank
p=0.026
0
2000
4000
6000
8000
Duration overall survival (days)
CHOL
Strata
group=Low
group=High
Survival probability
1.00
0.75
0.50
0.25
0.00
Log-rank
p=0.0042
0
500
1000
1500
2000
Duration overall survival (days)
LIHC
Strata
group=Low
group=High
Survival probability
1.00
0.75
0.50
0.25
0.00
Log-rank
p=0.0012
0
1000
2000
3000
4000
Duration overall survival (days)